EXPERIMENTAL AND MOLECULAR PATHOLOGY 25, 355–370 (1976)

Morphology and Morphogenesis of a Coronavirus Infecting Intestinal Epithelial Cells of Newborn Calves

A. M. DOUGHRI, J. STORZ, I. HAJER, AND H. S. FERNANDO

Department of Microbiology, College of Veterinary Medicine and Biomedical Sciences, Colorado State University, Fort Collins, Colorado 80523, and Department of Pathology, Arab Development Institute, Tripoli, Libya

Received April 26, 1976

The morphology and morphogenesis of virus strain LY-138 recovered from neonatal diarrheic calves were investigated by electron microscopy using negative-staining techniques and ultrathin sectioning. Purified viral particles were spherical in shape and measured 90 nm in average diameter in negatively stained preparations. Pleomorphic forms were also present. The virions had envelopes with petal-shaped projections characteristic of coronaviruses. In ultrathin sections, cores in viral factories were round with a diameter of 50–60 nm. Most of these cores were electron dense but some had an electron-lucent center. In cytoplasmic vacuoles, Golgi vesicles, and on the apical plasmalemma of intestinal epithelial cells, the virions were round or ellipsoidal in shape, measuring 70–80 nm in diameter, and had fine thread-like projections on their surfaces. Uptake of virus occurred through fusion of viral envelopes with the plasmalemma of the microvillous border or by entry into intercellular spaces and interaction with the lateral cell membranes of adjacent intestinal epithelial cells. As a result of this interaction, the lateral cell membranes became altered and ill-defined. During the early stage of infection, the rough and smooth elements of the endoplasmic reticulum became distended with electron-dense granulo-fibrillar material. This material accumulated subsequently as well-defined, smooth membrane-bound areas mainly in the apical cytoplasm of infected cells. These structures were considered to be viral factories. The morphogenesis of virus occurred mainly through condensation of the electron-dense, granulo-fibrillar material into viral cores in cytoplasmic viral factories or within the distended cisternae of the rough endoplasmic reticulum. Viral envelopment occurred on membranes of cytoplasmic vacuoles, Golgi vesicles, or in association with membranes of viral factories. Release of virus from infected cells occurred by lysis and fragmentation of the apical plasmalemma and flow of the cytoplasm with its contents into the gut lumen. Release also occurred by digestion and lysis of extruded infected cells or by fusion of virus-containing cytoplasmic vacuoles with the apical plasmalemma and liberation of their contents.

INTRODUCTION

Enteric diseases of neonatal animals represent serious economic and scientific problems. The infectious causes are diverse and include bacteria, viruses, and other agents (Storz *et al.*, 1970). A viral agent now identified as coronavirus strain LY-138 was recovered in 1965 from intestinal samples of diarrheic newborn calves. Several repeated attempts to adapt this viral agent to cultured bovine fetal kidney, lung, spleen, thyroid, and testicle cells were unsuccessful.

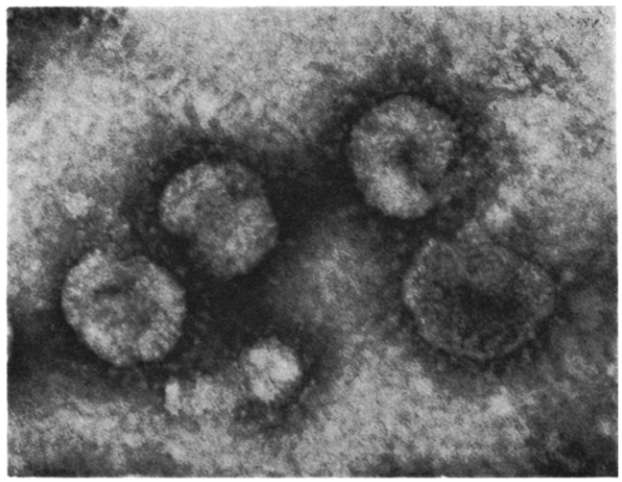

FIG. 1. Negatively stained viral particles of bovine coronavirus strain LY-138. Petal-shaped projections are evident. Internal structures are not detectable. ×170,000.

It is known that coronaviruses are difficult to adapt to cultured cells (McIntosh, 1974). Recently, Mebus and co-workers succeeded in adapting one bovine coranavirus strain to cultured bovine fetal kidney cells (Mebus *et al.*, 1974). Viral agent LY-138 was maintained by oral inoculation and intestinal infection of newborn calves. It induced consistently severe diarrhea in conventional calves. Since it was not possible to characterize this viral agent through methods provided by propagation in cell cultures, we explored some properties of this virus in the *in vivo* system of the original host.

The purpose of this study was to analyze the morphology and morphogenesis of coronavirus strain LY-138 as observed by electron microscopy after negative staining of purified virus or ultrathin sectioning of intestinal epithelial cells of experimentally infected newborn calves.

MATERIALS AND METHODS

Seven conventional neonatal calves were separated from their dams immediately after birth without access to colostrum. Each was kept in an isolation stall and was inoculated during the first 24 hr after birth. The initial inoculum was prepared from mucosal scrapings of a naturally infected diarrheic calf (LY-138). Intestinal samples of experimentally inoculated calves served as the viral source from which to prepare the inocula for subsequent experimental infections of calves. Intestinal mucosal scrapings were homogenized in Dulbecco's phosphate buffer to make a 10% homogenate. The homogenate was centrifuged at 3000*g* for 15 min to eliminate debris. The supernatant fluid was recovered and centrifuged at 17,300*g* for 30 min in a refrigerated centrifuge. The inoculum was prepared by diluting 70 ml of the second supernatant with Dulbecco's phosphate buffer to make 200 to 300 ml for each calf. The calves drank the inocula from nippled bottles.

Necropsy examination was performed when the calves reached a moribund stage 30 to 48 hr after inoculation. They were killed by electrocution. The ab-

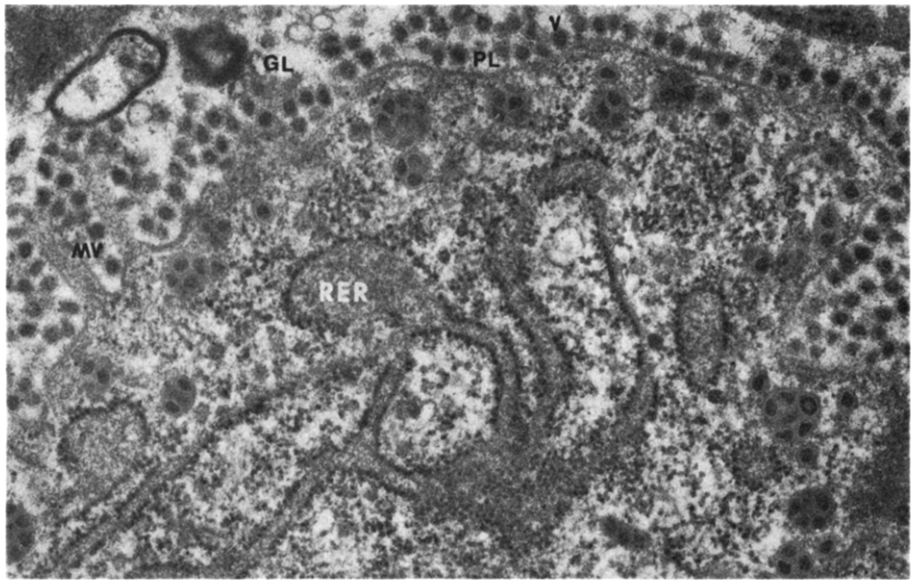

FIG. 2. Apical plasmalemma (PL) of intestinal absorptive epithelial cell lined with virions (V). Gut lumen (GL), microvilli (MV). Uranyl acetate–lead citrate stain. ×33,000.

dominal viscera were exposed at once. Intestinal samples were taken for viral and electron microscopic studies. Segments of 20-cm length of the different intestinal levels were frozen at −70°C.

Intestinal rings with a size of 2 mm were taken from the different parts of the intestinal tract and placed immediately into a petri dish containing ice-cold 6.25% phosphate-buffered glutaraldehyde at a pH of 7.2. As the tissue specimens became rigid after 4–5 min, they were cut into 1-mm^3 tissue blocks parallel to the longitudinal axis of the villi and prefixed for 2 hr. These specimens were then washed in phosphate-buffered saline and post-fixed for 1 hr in 1% osmium tetroxide as described by Millonig (1962). The tissue blocks were dehydrated and then embedded in Epon 812 by the procedure of Luft (1961). The tissue blocks were oriented in flat rubber molds to obtain sections parallel to the longitudinal axis of the microvilli. Ultrathin sections were cut with the MT-2B ultratome and were stained with uranyl acetate (Watson, 1958) followed by lead citrate (Reynolds, 1963).

Virus was purified from gut contents or mucosal scrapings in sucrose density gradients. A 10% homogenate in TEN buffer (0.01 *M* Tris–hydrochloride, 0.001 *M* EDTA, and 0.1 *M* NaCl) at pH 7.4 was centrifuged at 3000*g* for 15 min to sediment coarse particles. The supernatant was taken and recentrifuged at 12,000*g* for 30 min. The second supernatant was spun at 113,000*g* for 1 hr in an ultracentrifuge using an SW 40 rotor. The pellets were resuspended in 1 ml of 5% sucrose and overlayed on a 25–38% linear sucrose gradient and centrifuged at 81,000*g* for 2 hr. The bands were located by light scatter. The bands were collected from the bottom of the tubes and dialyzed overnight against 1% ammonium acetate at 4°C. The dialysate was concentrated to one-fifth of the original volume by extracting water with 40% polyethylene glycol. For negative staining, a drop of virus band was placed on a carbon–formvar-coated grid,

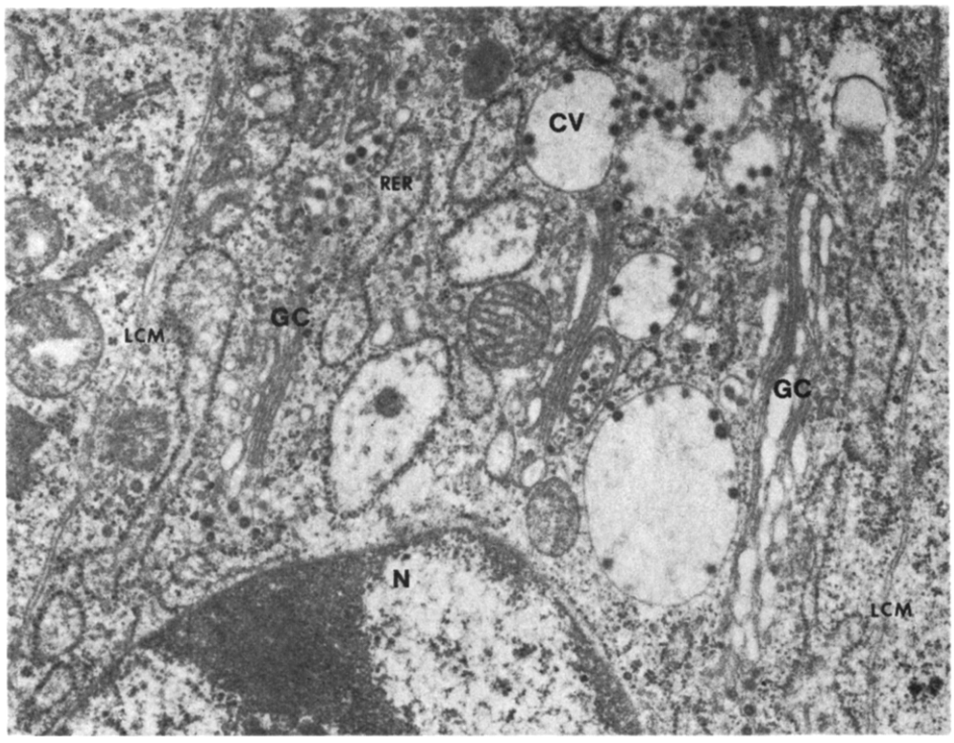

FIG. 3. Electron photomicrograph of intestinal absorptive epithelial cell. Cytoplasmic vacuoles (CV) are lined internally with viral particles. Golgi complexes (GC) and lateral cell membranes (LCM) are visible and the rough endoplasmic reticulum (RER) is dilated. Uranyl acetate–lead citrate stain. ×19,000.

allowed to air-dry, and then was stained with a drop of 2% potassium phosphotungstate at pH 6.5 for 1 min. Excess stain was removed with a filter-paper strip. The grids were allowed to air-dry at room temperature in a vacuum oven. All specimens were examined with an HU-12 Hitachi electron microscope at 75 kV. Magnifications were calibrated against carbon-grating replica having 2160 lines per millimeter (Ernest Fullam Co., No. 1002).

RESULTS

Morphology of Virion of Strain LY-138

The morphology of virions was assessed by negative staining of purified virus and in ultrathin sections. In negatively stained preparations the virions of strain LY-138 were enveloped and had a more or less spherical shape, but pleomorphic forms also existed. The overall diameter of the enveloped particle varied from 70 to 120 nm with an average of 90 nm. Viral cores were not seen in purified preparations. Widely spaced petal-shaped projections were seen on the envelopes. These projections measured from 150 to 200 Å in length and averaged 25 per virion circumference (Fig. 1).

In ultrathin sections, extracellular enveloped virions were free in the gut lumen or lined the apical plasmalemma of the intestinal epithelial cells. These viral

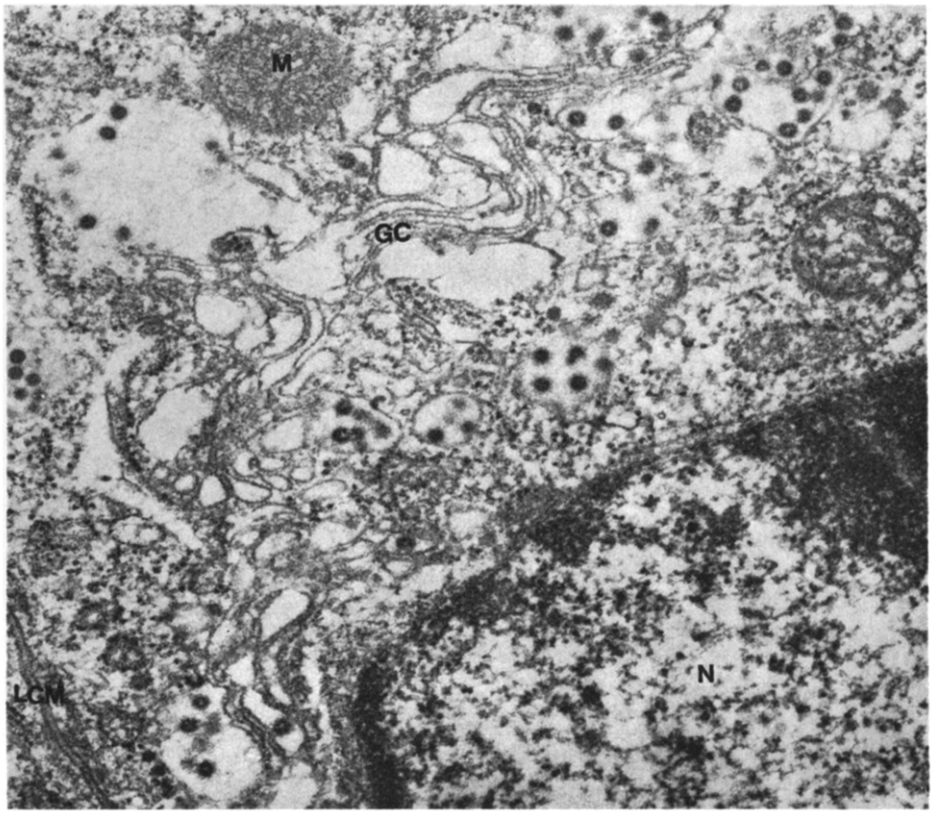

FIG. 4. Golgi complex (GC) involved in virus replication with dilated and vesiculated elements. Lateral cell membrane (LCM), mitochondrium (M), and nucleus (N). Uranyl acetate–lead citrate stain. ×30,700.

particles were round, measured 70 to 80 nm in diameter, and had electron-dense cores. Some of these virions had fuzzy, fine, thread-like surface projections. The inner leaflet of the trilaminar envelope was in intimate contact with the viral cores while the outer leaflet was separated by a narrow electron-lucent zone (Figs. 2, 5, and 12). Virions inside cytoplasmic vacuoles were round or ellipsoidal in shape, measuring 70 to 80 nm in diameter. The projections around the virions appeared as fine radiating threads at the periphery of some but not all of these virions (Fig. 3).

Two other morphologic viral structures were observed. One consisted of an electron-dense 50- to 60-nm core of differing electron density which was separated by a narrow electron-lucent halo from the less electron-dense background material. The second viral structure had a similar morphology but consisted of cores which had electron-lucent centers giving the appearance of doughnut-like structures (Figs. 4–6).

Morphogenesis of Virions of Strain LY-138

The uptake of the adsorbed virus particles occurred through the microvillous border of intestinal epithelial cells by fusion of viral envelopes with the plasma-

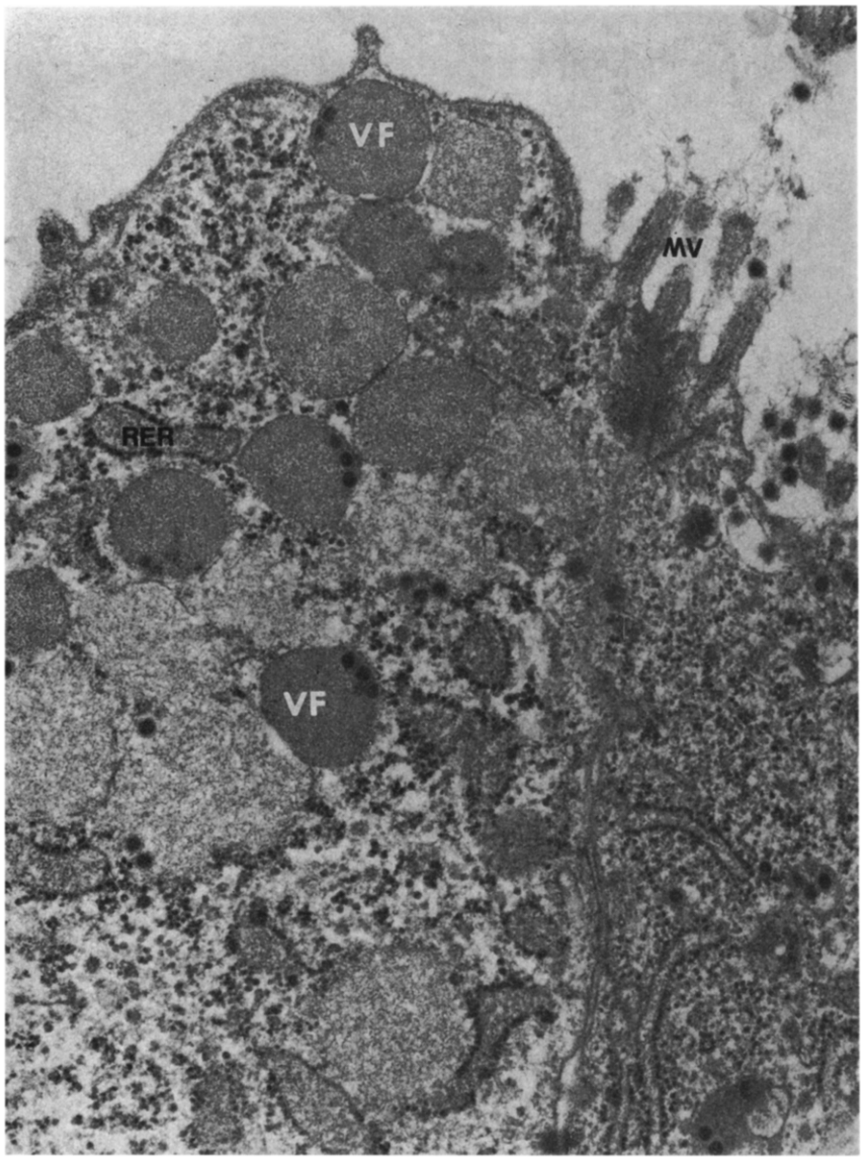

FIG. 5. Intestinal absorptive epithelial cell with dilated rough endoplasmic reticulum (RER) filled with electron-dense material. Membrane-bound viral factories (VF) containing electron-dense material with foci of viral core condensation. Microvilli (MV). Uranyl acetate–lead citrate stain. ×32,000.

lemma of the microvillous border or through entry into intercellular spaces and interaction with the lateral cell membranes which became altered and ill-defined at the site of viral contact (Figs. 7 and 8).

During the early stages of infection, there was an increase in the number of free ribosomes. Aggregates of single ribosomes were occasionally clustered around elements of the rough endoplasmic reticulum. No specific viral structures were associated with such aggregates. Distension of the cisternae of the rough and smooth endoplasmic reticulum with electron-dense granulo-fibrillar material was frequently seen (Fig. 9).

With the evident progression of replication, well-defined cytoplasmic structures containing electron-dense, granulo-fibrillar material appeared in the apical cytoplasm of infected intestinal epithelial cells. Some of these cytoplasmic structures were completely surrounded by a definite, smooth trilaminar membrane, while others were not (Figs. 5 and 13). These structures were considered to be viral factories. They were generally round in shape and ranged from 0.5 to 2.0 μm in diameter. Each factory contained homogenous, granulo-fibrillar material, and they varied in electron density. Viral structures at different stages of development were embedded in the matrices of viral factories. The number of these viral cores varied greatly in different viral factories, some of which contained no cores, some had few, while others were nearly filled with viral cores (Figs. 5, 6, and 13). The viral core structures had random arrangement in viral factories and never formed regular crystalline arrays. Coalescence of different viral

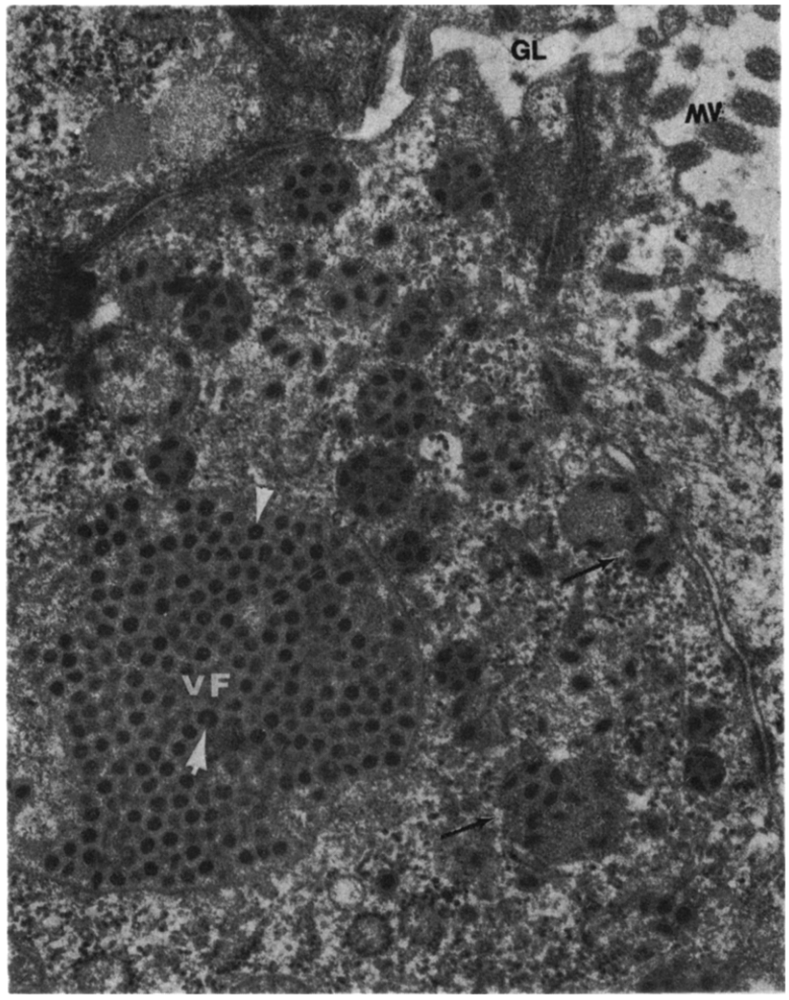

FIG. 6. Numerous viral factories (VF) in apical cytoplasm of intestinal absorptive epithelial cell with round, ellipsoidal, or doughnut-shaped (arrow head) viral cores. Smaller viral factories fuse (arrows). Gut lumen (GL) and microvilli (MV). Uranyl acetate–lead citrate stain. ×32,000.

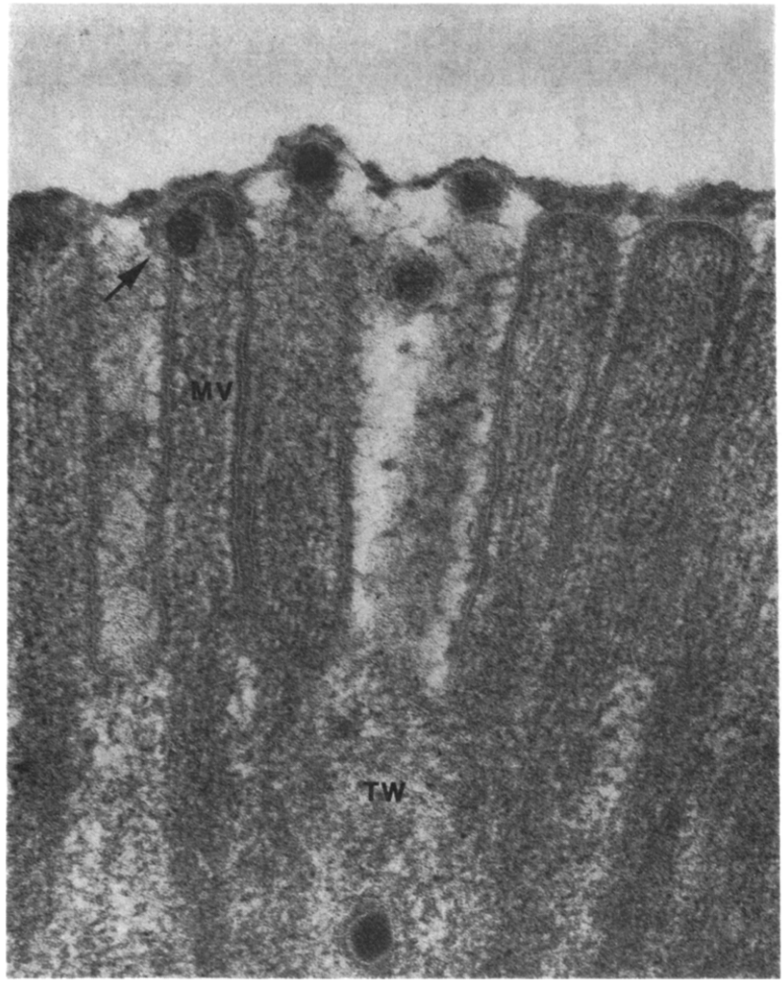

FIG. 7. Interaction of virions (arrow) with microvilli (MV) and terminal web (TW) in process of viral uptake by intestinal absorptive cell. Uranyl acetate–lead citrate stain. ×105,000.

factories occurred (Figs. 6 and 13). Viral core structures similar to those found in the viral factories were observed within electron-dense material of the distended cisternae of the rough endoplasmic reticulum. This electron-dense material resembled that present in viral factories (Fig. 10).

Some infected intestinal epithelial cells contained smooth-surfaced cytoplasmic vacuoles or Golgi vesicles lined internally with varying numbers of enveloped viral structures (Figs. 3 and 4). Golgi elements containing viral particles became vesiculated and dilated (Fig. 4). Occasionally, viral structures were observed free in the cytoplasmic matrix of degenerated infected cells.

Electron-dense, closely packed, convoluted tubules were infrequently seen in the cytoplasm of infected cells. Spherical forms comparable in size and density to the viral core structures were associated with this type of cytoplasmic inclusion (Fig. 11).

The apical plasmalemma of heavily infected cells underwent fragmentation and lysis and permitted the flow of cytoplasmic sol and its contents into the gut

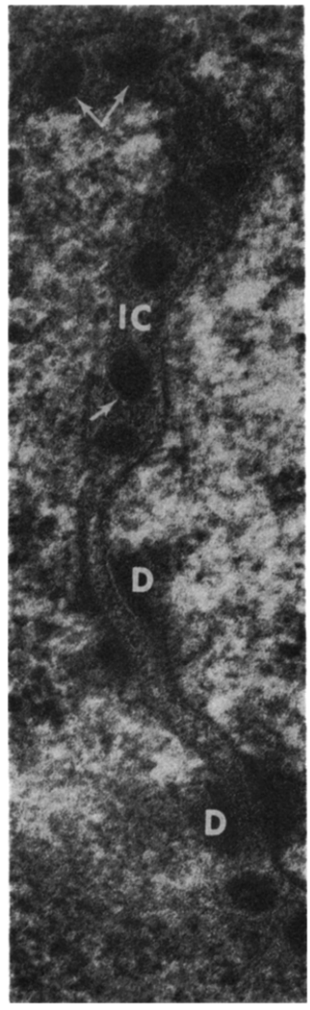

FIG. 8. Coronavirions (arrows) within intercellular space (IC) of adjacent intestinal epithelial cells. Desmosomes (D). Uranyl acetate–lead citrate stain. ×112,000.

lumen (Fig. 12). The limiting membrane of some virus-containing vacuoles fused with the apical plasmalemma of infected cells. The contents of these vacuoles were released into the extracellular environment (Fig. 13). Occasionally, entire infected cells or portions thereof were observed in the gut lumen. Digestion and lysis of these cells liberated virus (Fig. 14). The viral particles did not bud on the plasma cell membrane of infected cells. Large numbers of extracellular virus particles were observed singly or in clusters, lining the cell surfaces of normal-appearing and infected epithelial cells (Fig. 2). They were also present within the intercellular space of adjacent intestinal epithelial cells (Fig. 8).

DISCUSSION

Viral strain LY-138 consistently induced gastroenteritis in newborn calves and, apparently, is extremely fastidious in growing and adapting to cultured bovine cells. It was identified as a coronavirus by electron microscopic evalua-

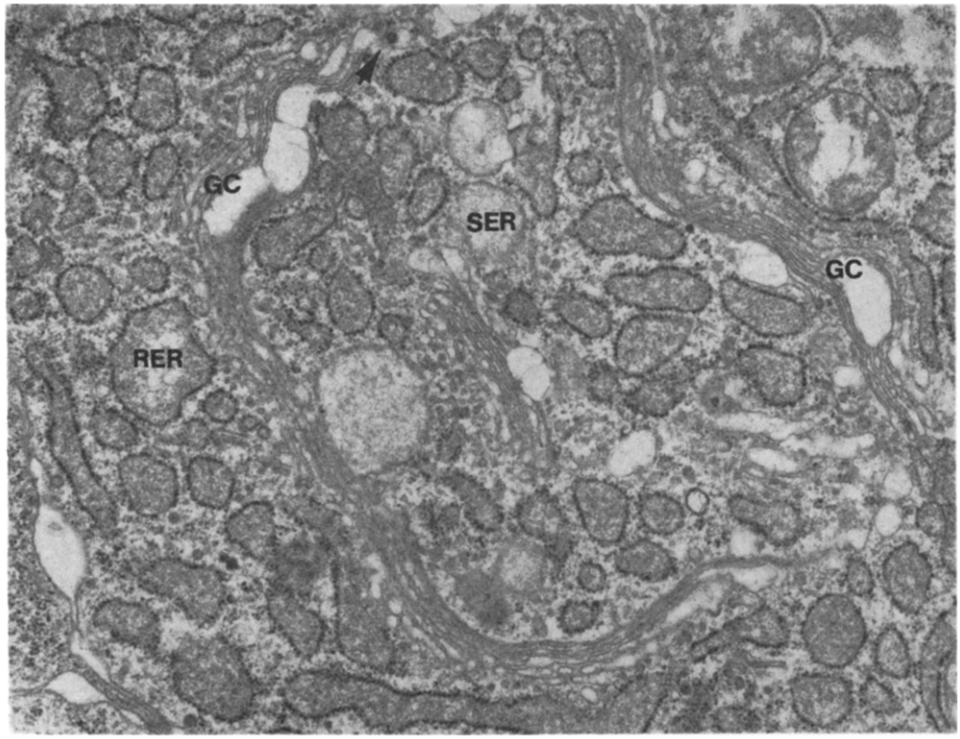

FIG. 9. Dilated rough (RER) and smooth (SER) endoplasmic reticulum filled with electron-dense material during early stage of infection with coronavirus. Golgi complexes (GC), virion in small Golgi vesicle (arrow head). Uranyl acetate–lead citrate stain. ×17,000.

tion of negatively stained preparations and ultrathin sections of infected intestinal epithelial cells. The size range, the presence of an envelope, and the characteristic petal-shaped surface projections characterized this viral strain as a coronavirus. The difference in size of the virus particles in negatively stained preparations and ultrathin sections can be attributed to the flattening of negatively stained virus particles and to shrinkage of tissue specimens during fixation and embedding. The majority of the intracellular virions has electron-dense cores, but occasionally, doughnut-shaped virus structures were observed in viral factories and in the dilated rough endoplasmic reticulum and Golgi vesicles.

Although intestinal epithelial cells were at various stages of infection, a general pattern of morphogenesis of the coronavirus strain LY-138 could be made since sequential morphologic cellular and viral changes were detectable. These changes were compared with the description of some morphologic features of replication of other coronaviruses which have been studied in different cultured cells (David-Ferreira and Manaker, 1965; Hamre *et al.*, 1967; Becker *et al.*, 1967; Okaniwa *et al.*, 1968; Nazarian and Cunningham, 1968; Oshiro *et al.*, 1971). Some of the cell lines used in these previous ultrastructural investigations expressed oncornaviruses which may complicate the analysis of the envelopment process of the coronavirus under study. Our *in vivo* system represented the highly specialized cell types infected in the naturally occurring disease, and the infected cells remained *in situ,* which permitted evaluation of the cellular topography and membrane response.

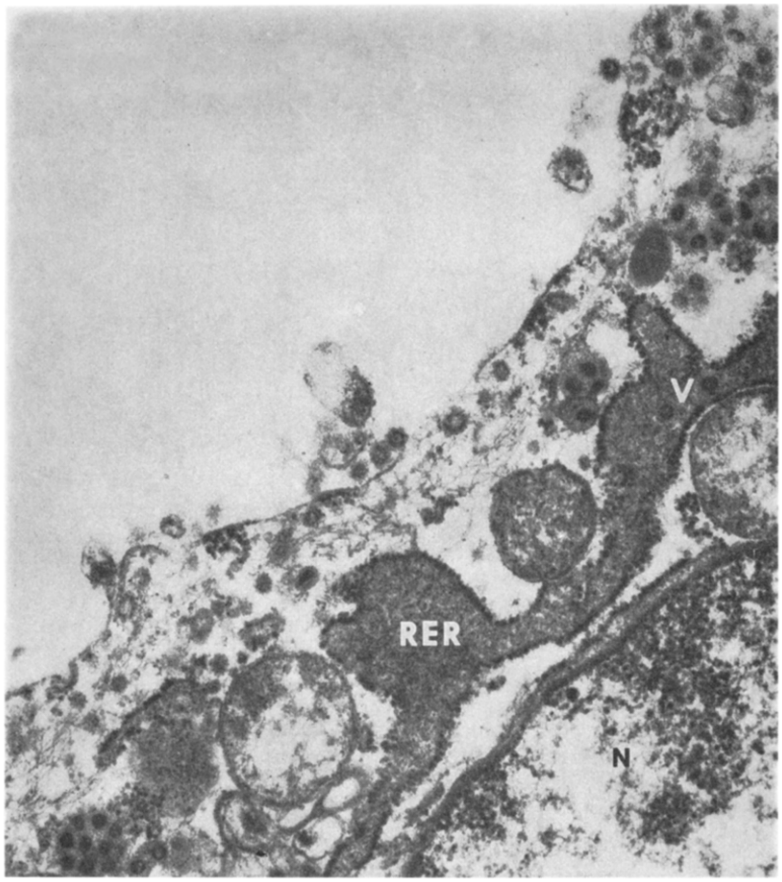

FIG. 10. Condensing viral cores (V) in electron-dense material with distended rough endoplasmic reticulum (RER). Nucleus (N). Uranyl acetate–lead citrate stain. ×32,000.

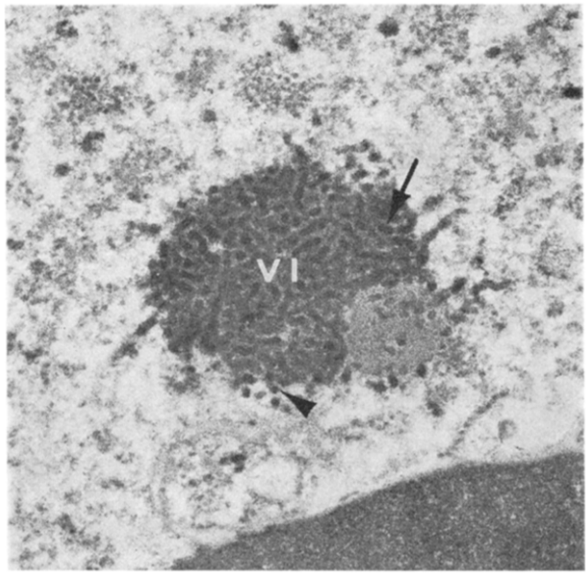

FIG. 11. Electron-dense, closely packed, convoluted viral inclusion (VI) in cytoplasm of intestinal absorptive epithelial cell. Evidence for beading (arrow) and cross section of tubules (arrow head). Uranyl acetate–lead citrate stain. ×38,000.

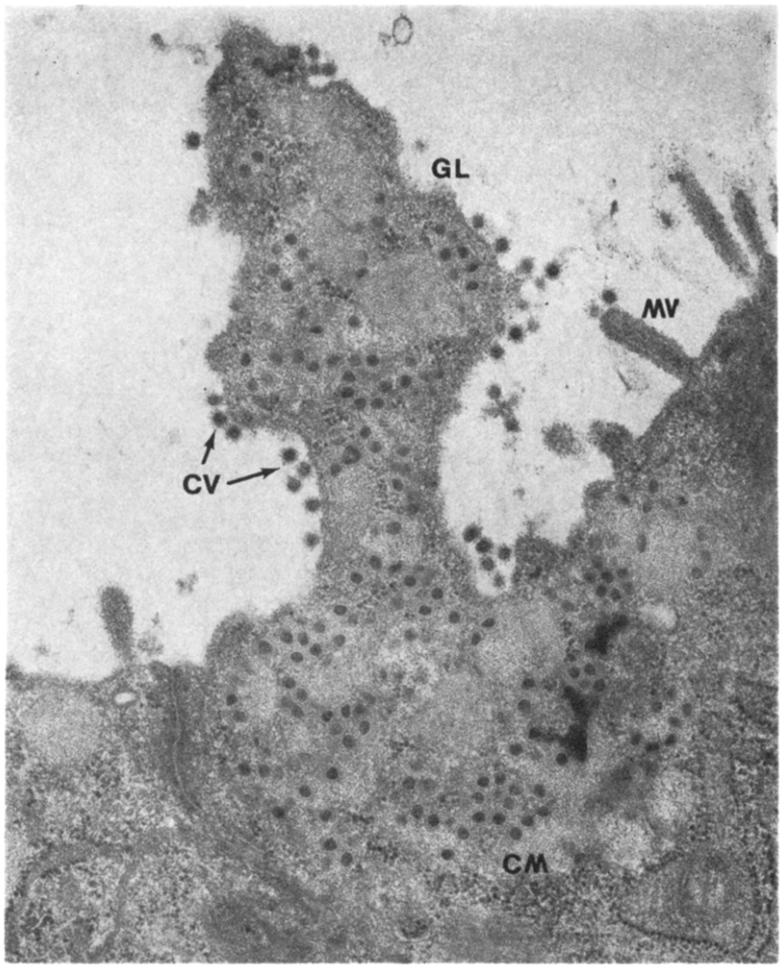

FIG. 12. Cytoplasmic matrix (CM) of infected intestinal absorptive epithelial cell flowing into the gut lumen (GL) with its contents and releasing virions (CV), microvilli (MV). Uranyl acetate–lead citrate stain. ×25,500.

Uptake of viral particles in intestinal infections occurred by fusion of the viral envelopes with the plasmalemma of the apical cell surface and by entry into intercellular spaces and interaction with lateral cell membranes.

The next phase of viral replication occurred in association with the elements of the endoplasmic reticulum network. The involvement of the rough and smooth endoplasmic reticulum in synthesis, processing, and assembly of viral structures was recognized in the replication of poliovirus (Caliguiri and Tamm, 1969), togavirus (Friedman *et al.*, 1972), and influenza virus (Campans, 1973; Lenard and Campans, 1974). The cisternae of the rough and smooth endoplasmic reticulum of coronavirus-infected intestinal epithelial cells became distended and filled with electron-dense material. Subsequently, viral factories, most of them lined with smooth membranes, emerged. This segregation of the viral factories appeared to be a function of the smooth endoplasmic reticulum. Viral cores were assembled by condensation of material in viral factories and of material within the rough endoplasmic reticulum. Membrane-bound, electron-dense cyto-

plasmic structures similar to the viral factories described here were present in electron photomicrographs of other studies on coronavirus replication. The role and involvement of the endoplasmic reticulum system in coronavirus replication were overlooked (David-Ferreira and Manaker, 1965; Hamre *et al.*, 1957; Oshiro *et al.*, 1971).

Our observations suggest that after core condensation, viral envelopment occurred in association with smooth membranes of viral factories, cytoplasmic vacuoles, or Golgi vesicles in the intestinal epithelial cells which we studied. Enveloped virions always lined the inner surfaces of the smooth membranes of the three vesicular structures mentioned. We never observed viral particles budding from membranes, as described by David-Ferreira and Manaker (1965). The cultured cells used by David-Ferreira and Manaker (1965) expressed oncornaviruses. The formation of definite viral cores in viral factories and envelopment in association with membranes would not conform with the stepwise viral assembly on membrane leading to the budding-off and release of mature coronavirions, as proposed by Becker *et al.* (1967). The Golgi complexes were involved in viral envelopment. Since viral cores were not seen to bud into this system, one has to postulate that the viral cores reached the Golgi elements through the channels of the endoplasmic reticulum system.

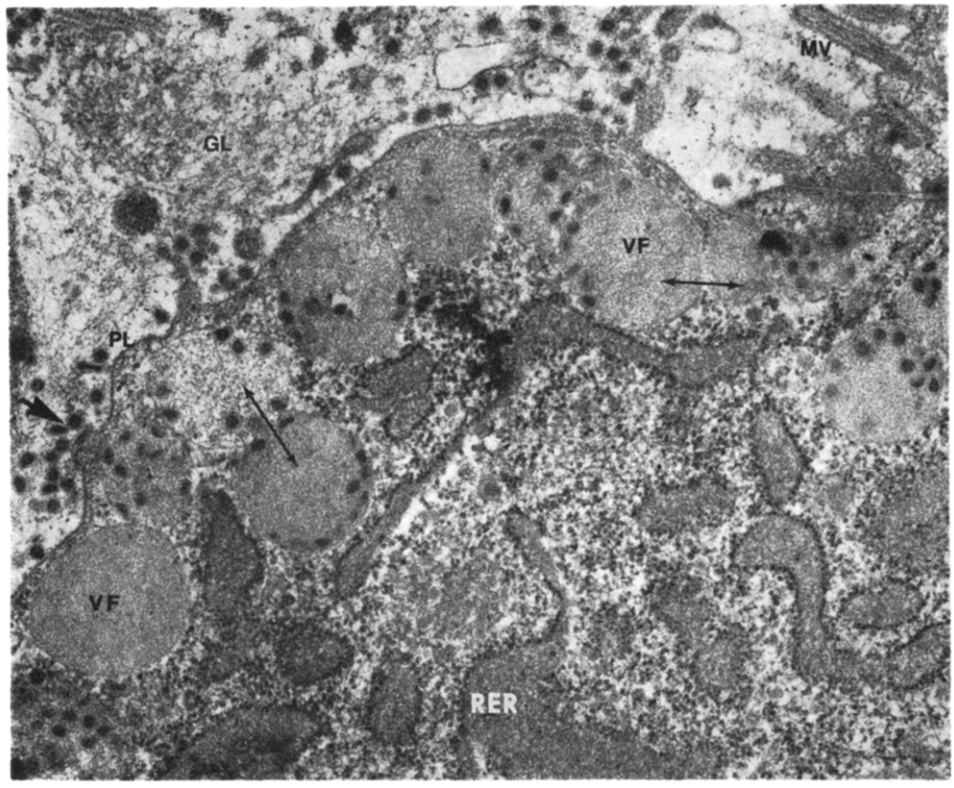

FIG. 13. Fragmented apical plasma cell membrane (PL) of intestinal epithelial cell releasing virus (arrow) into the gut lumen (GL). Viral factories (VF), their fusion (double-headed arrow) and distended rough endoplasmic reticulum (RER), microvilli (MV). Uranyl acetate–lead citrate stain. ×30,000.

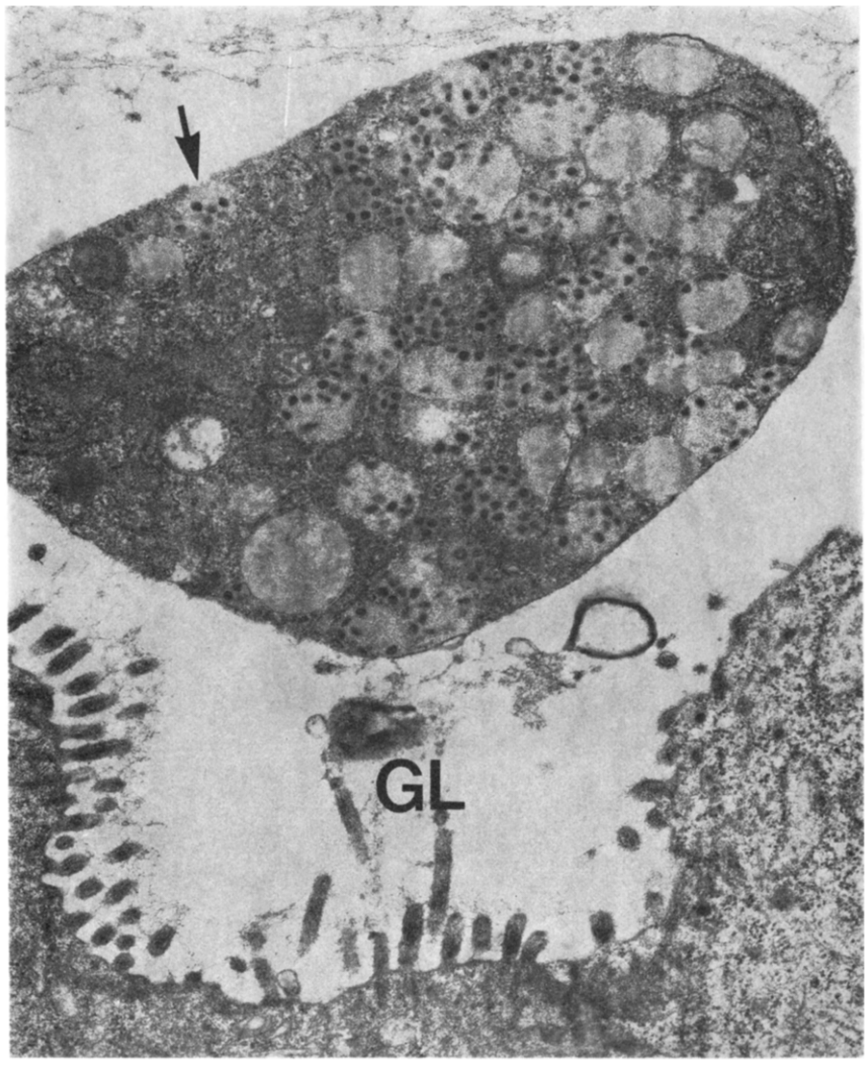

FIG. 14. Portion of infected intestinal absorptive epithelial cell in gut lumen (GL) releasing virus-containing vacuoles (arrow). Uranyl acetate–lead citrate stain. ×19,200.

Because of the observation that numerous enveloped viral particles attached to the plasmalemma of cell surfaces of normal and infected cells, others postulated that coronaviruses may become enveloped on cytoplasmic membranes (Witte *et al.*, 1968). Our observation did not indicate that plasma cell membranes were involved in coronavirus envelopment.

The significance of the occasionally observed electron-dense convoluted tubular structures is unknown. These were also described by David-Ferreira and Manaker (1965) and Oshiro *et al.* (1971).

Release of coronavirus from infected intestinal epithelial cells of calves occurred by lysis of the apical plasmalemma, through digestion and lysis of desquamated infected cells, or by fusion of virus-containing vacuoles with the apical plasmalemma and release of its contents into the gut lumen. The second mode of release was previously observed in infections of intestinal epithelial cells of piglets with the virus of transmissible gastroenteritis (Wagner *et al.*, 1973).

Our morphogenic studies indicated that this strain of bovine coronavirus appeared to be highly specific for intestinal epithelial cells. The high host-cell specificity could explain the lack of success in adapting this viral strain to cultured cells. Coronaviruses from other species have similar properties (McIntosh, 1974). Cultivation of intestinal epithelial cells *in vitro* probably will be necessary to provide the proper host cells for cultivation of this coronavirus strain.

ACKNOWLEDGMENTS

These investigations were supported by Regional Research Funds of Projects W-88 and W-120 and by funds from Jensen-Salsbery Laboratories, Kansas City, Missouri. This paper is published as scientific paper No. 2178, Colorado Agricultural Experiment Station. This work was initiated while J. Storz was associated with Utah State University.

We thank Mary L. Hegedus for skillful technical assistance.

REFERENCES

BECKER, W. B., MCINTOSH, K., DEES, J. H., and CHANOCK, R. M. (1967). Morphogenesis of avian infectious bronchitis virus and related human virus (strain 229E). *J. Virol.* **1**, 1019–1027.

CALIGUIRI, L. A., and TAMM, I. (1969). Membranous structures associated with translation and transcription of poliovirus RNA. *Science* **166**, 885–886.

COMPANS, R. W. (1973). Influenza virus proteins. II. Association with components of the cytoplasm. *Virology* **51**, 56–70.

DAVID-FERREIRA, J. F., and MANAKER, R. A. (1965). An electron microscope study of the development of a mouse hepatitis virus in tissue culture cells. *J. Cell Biol.* **24**, 57–78.

FRIEDMAN, R. M., LEVIN, J. G., GRIMLEY, P. M., and BEREZESKY, I. K. (1972). Membrane-associated replication complex in arbovirus infection. *J. Virol.* **10** (3), 504–515.

HAMRE, D., KINDIG, D. A., and MANN, J. (1967). Growth and intracellular development of a new respiratory virus. *J. Virol.* **1**, 810–816.

LENARD, J., and CAMPANS, R. W. (1974). The membrane structure of lipid-containing viruses. *Biochem. Biophys. Acta* **344**, 51–94.

LUFT, J. (1961). Improvements in epoxy resin embedding methods. *J. Biophys. Biochem. Cytol.* **9**, 409–414.

MCINTOSH, K. (1974). Coronaviruses: A comparative review. *Curr. Top. Microbiol. Immunol.* **63**, 85–129.

MEBUS, C. A., STAIR, E. L., RHODES, M. B., and TWIEHAUS, M. J. (1973). Neonatal calf diarrhea: Propagation, attenuation, and characteristics of a coronavirus-like agent. *Amer. J. Vet. Res.* **34**, 145–150.

MILLONIG, G. (1961). Advantages of a phosphate buffer for OsO_4 solutions in fixation. *J. Appl. Phys.* **32**, 1637.

NAZERIAN, K., and CUNNINGHAM, C. H. (1968). Morphogenesis of avian infectious bronchitis virus in chicken embryo fibroblasts. *J. Gen. Virol.* **3**, 469–470.

OKANIWA, A., HARADA, K., and KAJI, T. (1968). Electron microscopic investigation on the virus of transmissible gastroenteritis of pigs (Doyle and Hutchings, 1946) in infected tissue cultures. *Nat. Inst. Anim. Health Quart.* **8**, 148–163.

OSHIRO, L. S., SCHIEBLE, J. M., and LENNETTE, E. H. (1971). Electron microscopic studies of coronavirus. *J. Gen. Virol.* **12** (2), 161.

REYNOLDS, E. S. (1963). The use of lead citrate at high pH as an electron-opaque stain in electron microscopy. *J. Cell Biol.* **17**, 208–213.

STORZ, J., COLLIER, J. R., EUGSTER, A. K., and ALTERA, K. P. (1971). Intestinal bacterial changes in chlamydia-induced primary enteritis of newborn calves. *Ann. N.Y. Acad. Sci.* **176**, 162–175.

WAGNER, J. E., BEAMER, P. D., and RISTIC, M. (1973). Electron microscopy of intestinal epithelial cells of piglets infected with a transmissible gastroenteritis virus of pigs. *Canad. J. Comp. Med.* **37**, 177–188.

WATSON, M. L. (1958). Staining of tissue sections for electron microscopy with heavy metals. *J. Biophys. Biochem. Cytol.* **4**, 475–478.

WITTE, K. H., TAJIMA, M., and EASTERDAY, B. C. (1968). Morphologic characteristics and nucleic acid type of transmissible gastroenteritis virus of pigs. *Arch. Gesamte Virusforschung.* **23**, 53–70.